

Wind loads on curved canopy roofs

J Ginger¹, K Parackal¹, S Ingham¹, R Lowe¹ and C Hildebrandt¹

¹*Cyclone Testing Station, James Cook University, Townsville, Australia, john.ginger@jcu.edu.au*

SUMMARY:

The paper presents net wind pressures on a series of curved canopy roofs obtained by testing three 1/50 scale model configurations in a boundary layer wind tunnel. Large net negative (outward) and positive (inward) pressures were measured at the leading edges. Increasing positive net pressures were experienced especially on the windward parts of the roof with increasing curvature. Net pressure distributions generating peak horizontal and vertical loads on the frames will be used to produce net aerodynamic shape factors $C_{shp,n}$ in a form consistent with AS/NZS 1170.2 (2021).

Keywords: Wind load, curved canopy roof, net pressure, standard

1. INTRODUCTION

Curved, canopy roofs provide shade and accommodate open recreational spaces. Commonly, metal roof cladding is supported by purlins which are fixed to curved support frames. The gap between the roof and the ground typically ranges from 5m to 7m. There is limited wind load data to enable the cladding and the structural system in these types of roofs to be designed satisfactorily. Studies by Gumley (1981, 1982), Letchford and Ginger (1992) and Ginger and Letchford (1994) used models with sparsely spaced pressure taps to produce net pressure coefficients, $C_{p,n}$ for flat canopy roofs. AS/NZS1170.2 (2021) gives $C_{p,n}$ for mono-slope and pitched canopy roofs for pitch angles $\alpha = 0^\circ, 15^\circ$ and 30° and local pressure factors, K_l for designing cladding but their applicability for curved roofs may not be appropriate. This paper presents net wind pressures on a range of curved canopy roofs obtained from a wind tunnel model study, and will also provide these in the form consistent with AS/NZS1170.2 (2021).

2. WIND TUNNEL STUDY

The wind tunnel study was carried out in the 2.5m wide \times 2m tall \times 22m long Boundary Layer Wind Tunnel at the Cyclone Testing Station (CTS), James Cook University in Townsville, Australia. The approach Atmospheric Boundary Layer (ABL) was simulated at a length scale L_r of 1/50 over the upstream fetch using a 250 mm high trip board at the upstream end followed by an array of blocks on the tunnel floor to match the approach wind flow in a suburban terrain as specified in AS/NZS1170.2 (2021). The model to full scale velocity ratio, U_r is 2/5. Therefore, the model to full scale time ratio, $T_r = L_r/U_r = (1/50) \times (5/2) = 1/20$. Accordingly, a 10-min time interval in full scale is equivalent to 30 sec in model scale.

2.1. Roof configurations

Three open, curved canopy roof configurations described in Figure 1 and Table 1 were constructed at a Length scale, L_r of 1/50 and tested in the simulated atmospheric boundary layer flow. The profiles of the roofs were formed by circular arcs.

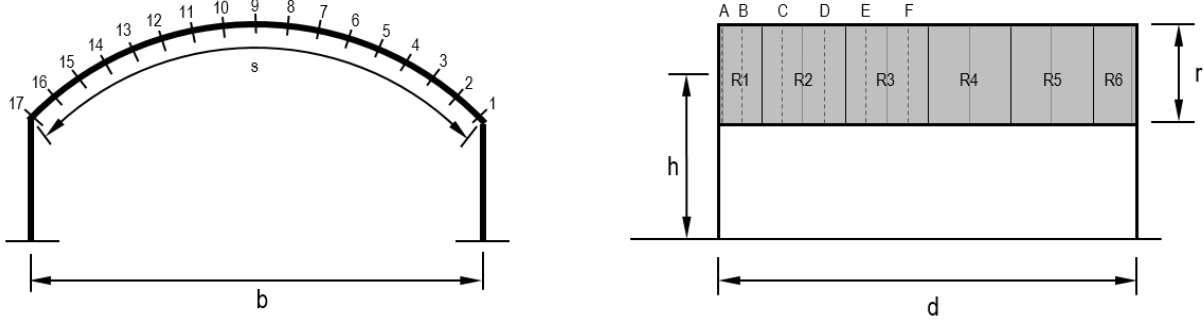


Figure 1. Open curved, canopy (i.e. free) roof building configurations

Table 1. Test Cases – Full scale dimensions

Case #	r (m)	h(m)	b (m)	d (m)	r/b	b/d
1	3.93	5.8	18.3	33.3	0.22	0.55
2	1.83	3.95	20.5	21	0.09	1.0
3	3	5.5	20	40	0.15	0.5

Pressure taps were installed on the top and bottom surfaces of the roofs on grids A1..17 to F1..17 defined by the location of frames and purlins on the roofs, as shown in Figure 1 for Cases 1, 2 and 3. Pressure fluctuations on the top ($p_T(t)$) and bottom, ($p_B(t)$) surface taps were measured for an observation time of 30 seconds at a frequency of 500 Hz and repeated three times for each wind direction from $\theta = 0^\circ$ to 355° at 5° intervals. The time (t) varying pressures are represented as pressure coefficients: $C_p(t) = (p(t) - p_o) / \frac{1}{2} \rho \bar{U}_h^2$ referenced to the mean dynamic pressure at mid-roof height, $\frac{1}{2} \rho \bar{U}_h^2$. Net pressure coefficients, $C_{pn}(t) = C_{pT}(t) - C_{pB}(t)$ were also generated at each pressure tap location.

The mean, maximum and minimum, pressure coefficients for each 30-second run are given by: $\bar{C}_p = (\bar{p} - p_o) / \frac{1}{2} \rho \bar{U}_h^2$, $\hat{C}_p = (\hat{p} - p_o) / \frac{1}{2} \rho \bar{U}_h^2$ and $\check{C}_p = (\check{p} - p_o) / \frac{1}{2} \rho \bar{U}_h^2$, where, \bar{p} , \hat{p} and \check{p} are the mean, maximum and minimum pressures in each 30 s time period \bar{U}_h is the mean wind speed at mid roof-height (h), ρ is the density of air and p_o is the ambient pressure. The data presented are based on the average values obtained from the three repeat runs for each approach wind direction. Design pressures can be derived from the C_{peak} wind tunnel test data (i.e. maximum and minimum pressure coefficient (\hat{C}_p, \check{C}_p)), and \bar{U}_h the equivalent 10-minute mean wind speed at the reference height h , and related to the aerodynamic shape factors C_{shp} in AS/NZS 1170.2 (2021). Here, $C_{shp} = (\bar{U}_h^2 / \hat{U}_h^2) C_{peak} = C_{peak} / G_u^2$, where $G_u = \hat{U}_h / \bar{U}_h$ is the velocity gust factor at the height h .

3 ANALYSIS & RESULTS:

3.1 Net Pressures

The net aerodynamic shape factors, $C_{shp,n}$ for cladding design for winds approaching from $\theta = 0^\circ \pm 45^\circ$ and $90^\circ \pm 40^\circ$ for Case 1 are given in Figure 2 and Figure 3, respectively. Figures 2a-b for $\theta = 0^\circ \pm 45^\circ$ show that the windward part of the roof (Taps 1-6) experiences positive net pressure coefficients. The central part of the roof (Taps 7-11), and the leeward part of the roof (Taps 12-17) experience negative net pressure coefficients. Figures 3a-b for $\theta = 90^\circ \pm 40^\circ$ show that the region near the windward edge of the roof (Grids A-B) experience large positive and negative net pressure coefficients, which accounts for application of local pressure factors $K_\ell > 1.0$ as noted in AS/NZS 1170.2 (2021). The net positive pressures tend to increase as the curvature of the roof increases from Case 2 to 3 to 1. The net negative pressures tend to increase in magnitude as the curvature of the roof decreases from Case 1 to 3 to 2.

Figure 2. Net aerodynamic shape factors $C_{shp,n}$, $\theta = 0^\circ \pm 45^\circ$, Case 1:

a) Maximum

	A	B	C	D	E	F
1	2.08	1.68	2.24	1.75	2.18	1.50
2	2.48	1.54	1.55	1.26	1.20	1.16
3	1.68	1.33	1.29	0.99	0.87	0.90
4	1.71	1.33	1.12	0.80	0.66	0.60
5	2.16	1.33	0.68	0.51	0.43	0.43
6	1.96	1.30	0.48	0.27	0.26	0.24
7	2.42	1.26	0.41	0.24	0.10	0.05
8	2.04	1.22	0.21	0.17	0.04	0.01
9	1.99	1.40	0.51	0.12	-0.04	-0.04
10	1.52	1.66	0.36	0.03	-0.06	0.05
11	1.04	0.83	0.36	0.04	-0.06	-0.02
12	0.82	0.48	0.41	0.12	-0.02	-0.07
13	0.77	0.55	0.21	0.05	0.06	0.09
14	0.63	0.45	0.34	0.26	0.23	0.19
15	0.54	0.47	0.37	0.32	0.40	0.24
16	0.86	0.45	0.44	0.31	0.30	0.26
17	0.61	0.40	0.53	0.31	0.40	0.29

b) Minimum

	A	B	C	D	E	F
1	-0.68	-0.59	-0.37	-0.50	-0.44	-0.48
2	-0.69	-0.29	-0.39	-0.27	-0.32	-0.33
3	-0.86	-0.38	-0.33	-0.42	-0.41	-0.42
4	-1.20	-0.38	-0.52	-0.46	-0.50	-0.62
5	-1.56	-0.49	-0.57	-0.58	-0.67	-0.70
6	-1.68	-0.66	-0.85	-0.73	-0.84	-0.85
7	-1.99	-0.78	-0.98	-0.98	-0.90	-1.05
8	-2.55	-0.92	-1.16	-1.03	-0.89	-0.91
9	-2.88	-1.09	-1.24	-1.17	-1.03	-0.97
10	-2.97	-1.41	-1.37	-1.25	-1.14	-1.08
11	-3.26	-1.93	-1.35	-1.36	-1.19	-1.13
12	-3.59	-1.77	-1.35	-1.31	-1.13	-1.13
13	-3.31	-2.00	-1.36	-1.24	-1.12	-1.10
14	-2.46	-2.02	-1.36	-1.18	-1.03	-1.04
15	-2.04	-1.99	-1.36	-1.06	-0.90	-0.81
16	-1.79	-1.84	-1.47	-1.06	-0.89	-0.74
17	-1.54	-1.41	-1.12	-0.90	-0.68	-0.64

Figure 3. Net aerodynamic shape factors $C_{shp,n}$, $\theta = 90^\circ \pm 40^\circ$, Case 1:

a) Maximum

	A	B	C	D	E	F
1	1.88	1.64	1.68	1.15	1.04	0.85
2	3.65	1.69	1.42	1.05	0.80	0.72
3	3.40	1.41	1.17	0.90	0.64	0.58
4	2.46	1.33	0.94	0.75	0.54	0.43
5	2.37	1.71	0.77	0.42	0.35	0.33
6	2.11	1.65	0.61	0.25	0.14	0.21
7	2.38	1.81	0.69	0.28	0.14	0.13
8	2.41	1.66	0.63	0.35	0.22	0.16
9	2.47	1.75	0.71	0.34	0.17	0.14
10	2.53	2.00	0.69	0.38	0.16	0.14
11	2.32	1.66	0.61	0.36	0.21	0.16
12	2.48	1.60	0.65	0.32	0.23	0.15
13	2.57	1.43	0.66	0.29	0.30	0.23
14	2.52	1.35	0.77	0.50	0.45	0.35
15	3.96	1.50	0.89	0.76	0.59	0.51
16	2.69	1.54	1.17	0.86	0.72	0.67
17	2.01	1.50	1.69	0.91	0.98	0.78

b) Minimum

	A	B	C	D	E	F
1	-2.65	-1.22	-0.91	-0.71	-0.66	-0.59
2	-2.36	-1.43	-1.39	-0.71	-0.89	-0.52
3	-2.17	-1.65	-1.12	-0.83	-0.76	-0.55
4	-2.35	-1.67	-1.03	-0.89	-0.70	-0.68
5	-2.82	-1.62	-0.93	-0.93	-0.78	-0.68
6	-2.98	-1.74	-0.94	-0.85	-0.82	-0.72
7	-2.97	-1.59	-0.95	-0.89	-0.78	-1.00
8	-2.72	-1.76	-1.06	-0.91	-0.81	-0.77
9	-2.59	-1.22	-1.07	-0.94	-0.95	-0.86
10	-2.95	-1.54	-1.03	-1.02	-0.97	-0.94
11	-3.30	-1.48	-1.02	-1.11	-0.95	-0.96
12	-3.25	-1.72	-0.97	-0.97	-0.95	-0.91
13	-2.58	-1.75	-1.02	-1.03	-0.95	-0.87
14	-2.55	-1.90	-1.06	-0.87	-0.89	-0.75
15	-2.30	-1.83	-1.21	-0.80	-0.79	-0.64
16	-2.27	-1.46	-1.40	-0.82	-0.76	-0.51
17	-2.82	-1.26	-1.04	-0.73	-0.59	-0.41

3.2. Roof Structural Loads

Net “area-averaged” pressures on Patches 1to17 on the roof tributary areas R1, R2 and R3 were used to obtain the structural loads, The time-varying loads acting on each patch are used to obtain load effects ($X(t)$) on each tributary area, in coefficient form C_x given by Equation 1.

$$C_x(t) = X(t)/\frac{1}{2}\rho\bar{U}_h^2 A_N; \quad X(t) = \left(\sum_{i=1}^N \beta_i A_i C_{pn_i}(t)\right) \times \frac{1}{2}\rho\bar{U}_h^2 \quad (1)$$

Here, β_i is the influence coefficient for the load applied at patch, i , A_i is the area for patch i , $C_{pn_i}(t)$ is the net pressure coefficient on patch, i at time t , N is the Number of patches on the tributary area influencing the load effect, X , A_N is the total area comprising the area of all patches within the tributary. The peak load effect coefficient (i.e. \widehat{C}_x , \check{C}_x) for horizontal force normal to building axis (H) and vertical force (V) for Case 1 are derived. The variation of peak (maximum and minimum) horizontal, H and vertical, V, load coefficients on each tributary area R1 with the approach wind direction for Case 1, are shown in Figure 4. These figures show that R1 experiences the largest horizontal loads, C_H for wind directions of about $\theta = 45^\circ$ and 135° . R1 experiences the largest upwards and downwards vertical loads, C_V for $\theta = 45^\circ$ to 135° .

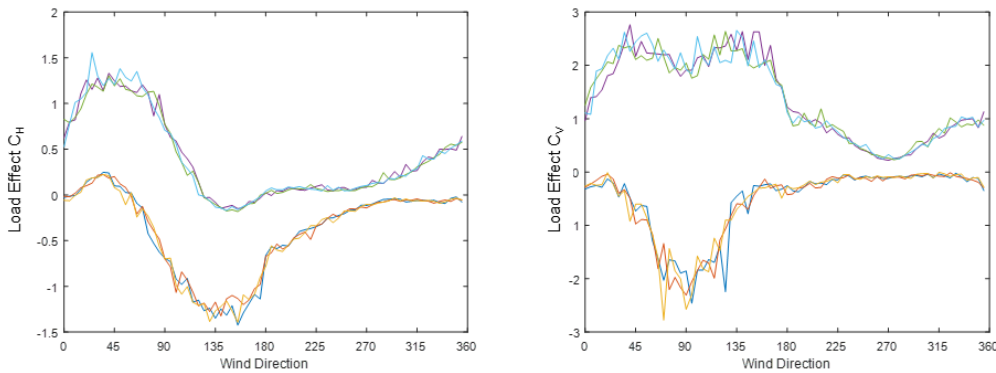


Figure 4. Maximum and minimum load effects; left: (C_H); right: (C_V) Case 1– Tributary R1

4 CONCLUSIONS

This paper shows that: Large net negative (outward) pressures net positive (inward) are experienced at the ends of the roof for oblique approach winds. Increasing curvature of the roof increases horizontal loads decreases vertical loads. The paper will also provide net pressures coefficients, $\widetilde{C}_{p,n}$, to be applied with the relevant area reduction factor K_a and local pressure factor K_l as in AS/NZS1170.2(2021) for the design of cladding and major structural elements

REFERENCES

- Gumley, S. J., (1981), “Panel loading mean pressure study for canopy roofs” Uni of Qxford, Dept of Engineering Science, OUEL Report No. 1380/81
- Gumley, S. J., (1982), “Design extreme pressures - A parametric study for canopy roofs” Uni of Qxford, Dept of Engineering Science, OUEL Report No. 1394/82.
- Standards Australia (2021), *Structural design actions. Part 2: wind actions*, Australian/New Zealand Standard, AS/NZS 1170.2:2021, Standards Australia, Sydney, New South Wales, Australia.
- Letchford C. W. and Ginger J. D., *Wind loads on planar canopy roofs, Part 1: mean pressure distributions*, Journal of Wind Engineering and Industrial Aerodynamics Vol 45, 1992, pp 25-45.
- Ginger J. D. and Letchford C. W., *Wind loads on planar canopy roofs, Part 2: fluctuating pressure distributions and correlations*, Journal of Wind Engineering and Industrial Aerodynamics Vol51, pp 353 – 370, 1994.